Appl. Phys. A 69 [Suppl.], S87–S93 (1999) / Digital Object Identifier (DOI) 10.1007/s003399900183

Applied Physics A
Materials
Science & Processing

Spherical expansion of the vapor plume into ambient gas: an analytical model

N. Arnold*, **J. Gruber, J. Heitz**

Angewandte Physik, Johannes-Kepler-Universität, Altenbergerstraße 69, 4040 Linz, Austria
(Fax: +43-732/2468-9242, E-mail: NIKITA.ARNOLD@JK.UNI-LINZ.AC.AT)

Received: 21 June 1999/Accepted: 1 September 1999/Published online: 22 December 1999

Abstract. A simplified model of plume expansion into ambient atmosphere is presented which is based on the laws of mass, momentum, and energy conservation. In the course of expansion, the energy is redistributed between the thermal and kinetic energies of the plume and (internal and external) shock waves (SW). The expansion is described by ordinary differential equations for the characteristic radii (contact surface, position of the SWs). The initial stage is similar to inertial expansion into vacuum, with radius $R \propto t$. Internal SW propagates inwards from the contact surface. Later expansion follows a point-blast model with $R \propto t^{2/5}$. Here the homogenized plume is decelerated and heated because of the counter-pressure of the ambient gas, which forms external SW. At a certain distance from the target, the plume stops (and even contracts), while external SW weakens and detaches from the contact surface. Analytical formulas for the transitional stages of expansion are discussed, and theoretical predictions are compared with experimental results of laser ablation of steel and YBCO in Ar.

PACS: 47.40.-x; 52.50.Jm; 42.62.-b

The dynamics of plume expansion is important for the pulsed-laser deposition (PLD) process and nanocluster formation. The expansion into vacuum can be described as self-similar and adiabatic [1, 2]. With higher ambient pressures, a point-blast model [1, 3] can be applied. At a certain distance from the target, the plume stops, while an external shock wave (SWe) weakens and detaches from the contact surface; later it degenerates into a sound wave.

The turnovers between these regimes have been studied numerically [4–6], but there are no satisfactory analytical formulas for the *transitional stages*. The drag model in [7] uses phenomenological fitting parameters. In [8] the plume (and the ambient gas) is subdivided into parts, which experience different numbers of collisions. Within the gas-dynamic picture, backscattered material forms an internal shock wave (SWi) [9]. This is a convenient framework for the description of experimentally observed heating of the leading edge of the plume [7] and plume splitting [10].

The formulas from the theory of explosions [11] have not been consistently applied to plume expansion. They mainly refer to the late stage of expansion, in which the plume is homogenized after SWi has traveled several times between the contact surface and the center. In [12] the (unrealistic) limiting case, in which all plume mass is in SWi, is considered. The models [13, 14] do not provide a detailed enough description of the transitional stages. In PLD, the buildup of SWe and the transition from the free adiabatic expansion to the point-blast behavior is slow. The proposed model bridges the gap between the analytical descriptions based on the free vacuum expansion and the strong-explosion models.

1 Model

We first introduce the notations. A schematic of the model is given in Fig. 1.

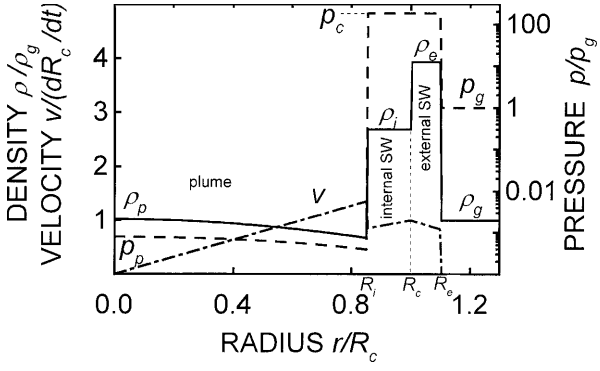

Fig. 1. Central part of the plume obeys free expansion laws. Densities (*solid line*) and pressures (*dashed line*) in the internal and external SW are assumed to be constant. Densities ϱ_i, ϱ_e obey corresponding SW conditions, while pressure p_c is equal to that at the contact boundary R_c and is found from the Newton's law for the external SW. Velocity distribution (*dash-dotted line*) is described in the text. Parameters are as in Fig. 2, $t = 0.4\left(\frac{M^5}{E^3\varrho_g^2}\right)^{1/6}$

*Corresponding author.

COLA'99 – 5th International Conference on Laser Ablation, July 19–23, 1999 in Göttingen, Germany

1.1 Notations

r – radial coordinate, t– time. Dot – derivative with respect to time; prime – derivative with respect to r. ζ_α denote different dimensionless coefficients. Their values, analytical and numerical, are given in Table 1.

Free plume (total): R– radius, M– mass, E– total energy, E_k – kinetic energy, E_t – thermal energy, ϱ_p – density profile, p_p – pressure profile, v_p – velocity profile, k – exponent in the density profile, v_f – inertial expansion velocity, γ_p – adiabatic exponent, R_0 – initial radius.

Central part of the plume, before internal SW: M_p – mass, E_pk – kinetic energy, E_pt – thermal energy. Internal SW: R_i – position (radius), M_i – mass, E_ik – kinetic energy, E_it – thermal energy, ϱ_i – density, p_i – pressure profile, v_i – velocity profile, R_c – position (radius) of the contact surface, p_c – pressure at the contact surface.

External SW: R_e – position (radius), M_e – mass, E_ek – kinetic energy, E_et – thermal energy, P_e – momentum, ϱ_e – density, p_e – pressure profile, v_{R_e} – gas velocity at the SW front, Ma_e – Mach number.

Ambient gas: ϱ_g – density, p_g – pressure, c_g – sound velocity, γ_g – adiabatic exponent.

1.2 Qualitative consideration and estimations

The overall energy in the *free* plume is conserved. For adiabatic expansion, the inertial stage is reached fast, where the $v_\mathrm{f} \sim (E/M)^{1/2}$ and almost all energy is kinetic.

In the presence of the ambient gas, the plume acts as a piston. Ambient gas is compressed and heated in the *external* SW. This adjoint mass decelerates the plume. At the same time, the ambient gas performs work on the plume and heats up it to a higher temperature than for expansion into the vacuum. The heating starts near the contact surface, where the molecules of the plume collide with the ambient molecules and are reflected. The *internal* SW is formed there and propagates inwards. This is inseparable from the deceleration of the plume, as the counter-pressure causes both. As the plume slows down, the SWi reaches the center, and a significant part of the plume energy becomes thermal. The SWi reflected from the center is weaker, i.e., the plume homogenizes.

Because the slowing of the plume is due to the adjoint mass, deviations from the free expansion occur when the mass of SWe is comparable with the plume mass: $M_\mathrm{e} \sim \varrho_\mathrm{g} R^3 \sim M$. The scales for this turnover are: $R_\mathrm{SW} \sim (M/\varrho_\mathrm{g})^{1/3}$, $t_\mathrm{sw} \sim R_\mathrm{SW}/v_\mathrm{f}$.

Table 1. Meanings, expressions, and values for different numerical coefficients. The abbreviation n.a. indicates that the information is not available.

Co.	Meaning		Formula	See Eq. #	Values: $\gamma_\mathrm{p}=5/3$, $\gamma_\mathrm{g}=5/3$	
					Formula	Numerical
ζ_i	Plume homogenization	Radius	n.a.	(20)	n.a.	0.83 ($k=3/2$) 0.66 ($k=0$)
ζ_ti		Time	n.a.	(20)	n.a.	0.87 ($k=3/2$) 0.59 ($k=0$)
ζ_M		Mass ratio M_e/M	$\frac{2\pi}{3}(\gamma_\mathrm{g}+1)\zeta_\mathrm{i}^3$	(20)	n.a.	3.22 ($k=3/2$) 1.64 ($k=0$)
ζ_c		radii ratio R_c/R	$\left(\frac{3\pi^{1/2}}{4}\frac{\gamma_\mathrm{p}-1}{\gamma_\mathrm{p}+1}\frac{\Gamma(k+1)}{\Gamma(k+5/2)}\right)^{1/3}$	(20)	0.42 0.63	0.41 ($k=3/2$) 0.62 ($k=0$)
ζ_E	Kinetic energy of the strong external SW, $E_\mathrm{ek}=\frac{\zeta_E}{2}M_\mathrm{e}\dot{R}_\mathrm{c}^2$		$\frac{1}{3}\left(\left(\frac{\gamma_\mathrm{g}+1}{2}\right)+\left(\frac{\gamma_\mathrm{g}+1}{2}\right)^{1/3}+\left(\frac{\gamma_\mathrm{g}+1}{2}\right)^{-1/3}\right)$	(22)	1.114	1.107
ζ_P	Momentum of the strong external SW, $P_\mathrm{e}=\zeta_P M_\mathrm{e}\dot{R}_\mathrm{c}$		$\frac{1}{2}\left(\left(\frac{\gamma_\mathrm{g}+1}{2}\right)+\left(\frac{\gamma_\mathrm{g}+1}{2}\right)^{1/3}\right)$	(22)	1.217	1.213
ζ_A	Coefficients in the eq. (23)	Kinetic energy	$\frac{2\pi}{3}\zeta_E\gamma_\mathrm{g}$	(23)	3.89	n.a.
ζ_B		Thermal energy	$\frac{2\pi}{9}\frac{\gamma_\mathrm{p}+1}{\gamma_\mathrm{p}-1}\zeta_P\gamma_\mathrm{g}$	(23)	5.66	n.a.
ζ_C		Initial thermal energy	$\frac{2\pi}{3}\left(\frac{\gamma_\mathrm{p}+1}{\gamma_\mathrm{p}-1}\left(\frac{\gamma_\mathrm{g}+1}{2}\right)^{2/3}-\frac{\gamma_\mathrm{g}+1}{\gamma_\mathrm{g}-1}\right)$	(23)	1.77	n.a.
ζ_{R_SW}	Equation for the free plume-strong SW transition	Radius	$\left(\frac{20\pi}{9}\left(\zeta_E+\frac{\zeta_P}{2}\frac{\gamma_\mathrm{p}+1}{\gamma_\mathrm{p}-1}\right)\right)^{-1/3}$	(24)	0.35	n.a.
ζ_{t_SW}		Time	$\zeta_{R_\mathrm{SW}}\left(\frac{3}{10}\right)^{1/2}$	(24)	0.19	n.a.
$\zeta_{R\mathrm{st}}$	Equation and parameters for the plume stopping	Radius	$\left(\frac{2(\zeta_A+3\zeta_\mathrm{b})}{\zeta_C(2\zeta_A+3\zeta_B)}\right)^{1/3}$	(25)	0.98	0.39
ζ_{t_st1}		Time	$\left(\frac{2^2(\zeta_A+3\zeta_\mathrm{b})^5}{\zeta_C^5(2\zeta_A+3\zeta_B)^2}\right)^{1/6}$	(25)	3.38	n.a.
ζ_{t_st}		Stopping time	$\frac{1}{3}B_1\left(\frac{5}{6},\frac{1}{2}\right)\zeta_{t_\mathrm{st1}}$	(26)	2.52	0.31
ζ_e		Ratio $R_\mathrm{e}/R_\mathrm{c}$	n.a.	(26)	n.a.	1.77

If the thermal energy of the plume is high when $M_e > M$, expansion follows the point-blast model: $R \sim (Et^2/\varrho_g)^{1/5}$. As long as SWe remains strong, the contact boundary and SWe are close to each other. The expansion is not completely adiabatic at this stage. The pressure within the (homogeneous) plume further decreases, and SWe weakens and detaches from the contact surface. The pressure becomes comparable to the ambient pressure $p \sim (E^2\varrho_g^3/t^6)^{1/5} \sim p_g$, the expansion velocity becomes comparable to the sound velocity in the ambient $\dot{R} \sim (E/\varrho_g t^3)^{1/5} \sim (p_g/\varrho_g)^{1/2}$, and the initial thermal energy of the gas involved in SWe becomes comparable with the initial energy of the plume $p_g R^3 \sim E$. Any of these conditions yields for the stopping of the contact boundary: distance $R_{st} \sim (E/p_g)^{1/3}$ time $t_{st} \sim (E/p_g)^{1/3}/c_g$. One can see that $R_{st}/R_{SW} \sim (v_f/c_g)^{2/3}$. Thus, the strong-explosion model is relevant only if $v_f \gg c_g$. Below we develop a unified model for all these stages, as well as a description for the *transitional* regions: free expansion – strong SW, and strong SW – stopping of the plume.

1.3 Basic assumptions and factors not taken into consideration

We assume that the equations of gas dynamics can be applied. We do not consider Knudsen-layer effects; i.e., typical length scales are bigger than the mean free path. In [8] the plume is subdivided into parts experiencing 1, 2, or more collisions. Even with low pressures, it is necessary to sum 5–10 collisions; this justifies our approach.

The contact boundary is treated as an impenetrable reflecting piston, thus mixing between the expanding plume and the ambient gas is *not* considered. In PLD, the initial stage of expansion is close to one-dimensional (1D), which is not discussed here. We also do not consider the initial stage of the *spherical* expansion with $R \sim R_0$. It can be incorporated, but with loss in the simplicity of the description.

We assume a *spherical* symmetry. For the *semispherical* expansion, E and M are the *doubled* energy and mass of the plume. E is the initial energy of the *plume* and does not include losses on the sample heating, evaporation, etc. The determination of E and M is a separate problem. Condensation, recombination of charged species, excitation of the internal degrees of freedom, and so forth are not considered. Their incorporation changes the form of energy conservation.

1.4 Main equations

For a simplified analysis, we use the conservation laws derived from gas dynamic equations, and the assumptions about the profiles of thermodynamic variables. This results in the equations for four dynamic variables, R_i, R_c, R_e, and R. The key approximation is that the densities and pressures in SW do not depend on r.

Free plume expansion follows from the *conservation of its energy* (kinetic plus thermal):

$$E_k(M, \dot{R}) + E_t(E, R, R_0) = E \,. \tag{1}$$

Mass conservation within the plume with *strong* SWi yields an explicit (nondifferential) equation for R_i:

$$M_p(R_i, R) + M_i(R_c, R_i, R) = M \,. \tag{2}$$

Mass conservation in the external SW yields the differential equation for R_e:

$$M_e(R_c, R_e, \varrho_e(\dot{R}_e)) = M_{\text{ambient}}(R_e, \varrho_g) \,. \tag{3}$$

The expansion dynamics follows the *overall energy conservation* (differential equation for R_c). We indicate the variables that are important for the corresponding energies.

$$E_{pk}(R_i, R, \dot{R}) + E_{pt} + E_{ik}(R_i, R_c, R, \dot{R}_c) + E_{it}(R_i, R_c, p_c) + E_{ek}(R_c, R_e, \dot{R}_c, \dot{R}_e) + E_{et}(R_c, R_e, p_c) = E \,. \tag{4}$$

With a spatially homogeneous pressure within SW, E_{it} and E_{et} are determined by the contact pressure p_c. It is found from *Newton's law for the external SW*:

$$\frac{d}{dt}\left[P_e(R_c, R_e, \dot{R}_c, \dot{R}_e)\right] = 4\pi R_c^2 p_c - 4\pi R_e^2 p_g \,. \tag{5}$$

If P_e is exact, this equation is exact. It follows from the flow of momentum through a spherical layer and gas dynamic equations. p_c must be then substituted in (4). The equations (2)–(4) require the initial conditions:

$$R_i(0) \approx R_c(0) \approx R_e(0) \approx R(0) \approx R_0, \qquad \dot{R}_c(0) \approx \dot{R}_c(0) = v_f(E, M) \,, \tag{6}$$

R_0 being a small quantity. Numerical subtleties related to (6) will be described elsewhere. Below we write the simplified expressions for the masses, energies, and momentum for the different parts of the plume-SW system.

2 Equations

2.1 Free plume

Without an ambient atmosphere, the plume expands adiabatically in a self-similar fashion [1, 2]. Density and pressure profiles, which satisfy equations of gas dynamics with velocity $v_p = \dot{R}r/R$ are (with the initial plume at rest):

$$\varrho_p = \frac{\Gamma(k+5/2)}{\pi^{3/2}\Gamma(k+1)}\frac{M}{R^3}\left(1-\left(\frac{r}{R}\right)^2\right)^k \,,$$
$$p_p = (\gamma_p - 1)\frac{\Gamma(k+7/2)}{\pi^{3/2}\Gamma(k+2)}\frac{E}{R_0^3}\left(\frac{R_0}{R}\right)^{3\gamma_p}\left(1-\left(\frac{r}{R}\right)^2\right)^{k+1} \,. \tag{7}$$

Here Γ is the Gamma function. The entropy decreases from the center if $k < 1/(\gamma_p - 1)$. The energy conservation (1) takes the form:

$$E_k + E_t \equiv \frac{3}{4k+10}M\dot{R}^2 + E\left(\frac{R_0}{R}\right)^{3(\gamma_p-1)} = E \,. \tag{8}$$

After a short time, with R of the order of several R_0, the plume expands inertially, with

$$\dot{R} \equiv v_f = \sqrt{\frac{4k+10}{3}\frac{E}{M}} \,. \tag{9}$$

In the inertial stage, the thermal energy density is much less than the kinetic-energy density.

2.2 Central part of the plume

The central part of the plume, before SWi ($r < R_\mathrm{i}$), is unaffected by the ambient gas. The mass and the energies within this part of the plume follow from (7) and can be expressed via the hypergeometric function ${}_2F_1$:

$$
\begin{aligned}
M_\mathrm{p} &\equiv \int_0^{R_\mathrm{i}} \varrho_\mathrm{p} 4\pi r^2 \,\mathrm{d}r = \frac{4}{3\pi^{1/2}} \frac{\Gamma(k+5/2)}{\Gamma(k+1)} \left(\frac{R_\mathrm{i}}{R}\right)^3 \\
&\quad \times {}_2F_1\left[\frac{3}{2}, -k, \frac{5}{2}, \left(\frac{R_\mathrm{i}}{R}\right)^2\right] M \,, \\
E_\mathrm{pk} &\equiv \int_0^{R_\mathrm{i}} \varrho_\mathrm{p} \frac{v_\mathrm{p}^2}{2} 4\pi r^2 \,\mathrm{d}r \\
&= \frac{2(4k+10)}{15\pi^{1/2}} \frac{\Gamma(k+5/2)}{\Gamma(k+1)} \left(\frac{R_\mathrm{i}}{R}\right)^3 \\
&\quad \times {}_2F_1\left[\frac{5}{2}, -k, \frac{7}{2}, \left(\frac{R_\mathrm{i}}{R}\right)^2\right] E \,, \\
E_\mathrm{pt} &\equiv \int_0^{R_\mathrm{i}} \frac{p_\mathrm{p}}{\gamma_\mathrm{p}-1} 4\pi r^2 \,\mathrm{d}r \approx 0 \,.
\end{aligned} \tag{10}
$$

The last equalities for the energies assume an inertial stage of expansion. The pressure within the plume can be omitted from the calculations of the overall energy, as it is much lower than the plume kinetic-energy density. For this reason, SWi propagating within the plume is considered as *strong* SW.

2.3 Internal SW

The plume material which is reflected from the contact surface forms SWi. We adopt a velocity profile: $v_\mathrm{i} = \dot{R}_\mathrm{c} r / R_\mathrm{c}$. Such a choice, though not correct near $r \sim R_\mathrm{i}$, describes the homogeneous plume from the moment when SWi reaches the center. The details of the velocity profile do not significantly affect the result. The mass of SWi is given by:

$$
\begin{aligned}
M_\mathrm{i} &\equiv \int_{R_\mathrm{i}}^{R_\mathrm{c}} \varrho_\mathrm{i} 4\pi r^2 \,\mathrm{d}r = \frac{4\pi}{3} \left(R_\mathrm{c}^3 - R_\mathrm{i}^3\right) \varrho_\mathrm{i} \\
&= \frac{4\pi}{3} \left(R_\mathrm{c}^3 - R_\mathrm{i}^3\right) \frac{\gamma_\mathrm{p}+1}{\gamma_\mathrm{p}-1} \varrho_\mathrm{p}(R_\mathrm{i}) \,.
\end{aligned} \tag{11}
$$

Here, the density ϱ_i is assumed to be r-independent and related to $\varrho_\mathrm{p}(R_\mathrm{i})$ via the *strong*-SWi condition. $\varrho_\mathrm{p}(R_\mathrm{i})$ is given by (7) with $r = R_\mathrm{i}$. With M_p from (10) and M_i from (11), the mass conservation (2) is given by:

$$
\begin{aligned}
&\left[\left(\frac{R_\mathrm{i}}{R}\right)^3 {}_2F_1\left[\frac{3}{2}, -k, \frac{5}{2}, \left(\frac{R_\mathrm{i}}{R}\right)^2\right] + \frac{\gamma_\mathrm{p}+1}{\gamma_\mathrm{p}-1} \left(\frac{R_\mathrm{c}^3 - R_\mathrm{i}^3}{R^3}\right) \right. \\
&\qquad \left. \times \left(1 - \left(\frac{R_\mathrm{i}}{R}\right)^2\right)^k \right] \frac{4}{3\pi^{1/2}} \frac{\Gamma(k+5/2)}{\Gamma(k+1)} M = M \,.
\end{aligned} \tag{12}
$$

This equation defines the position of SWi, R_i. With $v_\mathrm{i} = \dot{R}_\mathrm{c} r / R_\mathrm{c}$ and $\varrho_\mathrm{i}[\varrho_\mathrm{p}(R_\mathrm{i})]$, the energies are:

$$
\begin{aligned}
E_\mathrm{ik} &\equiv \int_{R_\mathrm{i}}^{R_\mathrm{i}} \varrho_\mathrm{i} \frac{v_\mathrm{i}^2}{2} 4\pi r^2 \,\mathrm{d}r = \frac{2\pi}{5} \varrho_\mathrm{i} \dot{R}_\mathrm{c}^2 \left(\frac{R_\mathrm{c}^5 - R_\mathrm{i}^5}{R_\mathrm{c}^2}\right) = \frac{2}{5\pi^{1/2}} \\
&\quad \times \frac{\gamma_\mathrm{p}+1}{\gamma_\mathrm{p}-1} \frac{\Gamma(k+5/2)}{\Gamma(k+1)} \left(\frac{R_\mathrm{c}^5 - R_\mathrm{i}^5}{R_\mathrm{c}^2 R^3}\right) \left(1 - \left(\frac{R_\mathrm{i}}{R}\right)^2\right)^k M \dot{R}_\mathrm{c}^2 \,, \\
E_\mathrm{it} &\equiv \int_{R_\mathrm{i}}^{R_\mathrm{i}} \frac{p_\mathrm{i}}{\gamma_\mathrm{p}-1} 4\pi r^2 \,\mathrm{d}r = \frac{4\pi}{3} \left(R_\mathrm{c}^3 - R_\mathrm{i}^3\right) \frac{p_\mathrm{c}}{\gamma_\mathrm{p}-1} \,.
\end{aligned} \tag{13}
$$

We assume that when SWi reaches the center, the plume becomes homogeneous. In reality, SWi travels several times between the center and the contact surface. At this stage it weakens [11], and the assumption of a homogeneous plume is not a bad one [4, 6].

2.4 External SW

The ambient gas compressed by the expanding plume forms SWe. We approximate the velocity in this region by a linear function: between $\dot{R}_\mathrm{c}$ at R_c, and v_{R_e} at R_e. v_{R_e} and the (constant) density in SWe are found from the condition at the front of SWe:

$$
\begin{aligned}
v_{R_\mathrm{e}} &= \frac{2\dot{R}_\mathrm{e}}{\gamma_\mathrm{g}+1} \left(1 - Ma_\mathrm{e}^{-2}\right) , \\
\varrho_\mathrm{e} &= \frac{\gamma_\mathrm{p}+1}{\gamma_\mathrm{p}-1} \left(1 + \frac{2Ma_\mathrm{e}^{-2}}{\gamma_\mathrm{g}-1}\right)^{-1} \varrho_\mathrm{g}, \quad Ma_\mathrm{e} \equiv \frac{\dot{R}_\mathrm{e}}{c_\mathrm{g}} \,.
\end{aligned} \tag{14}
$$

The gas in SWe originally occupied the volume currently encompassed by R_e. If $R_0 \ll R_\mathrm{e}$, the mass conservation (3) becomes:

$$
M_\mathrm{e} \equiv \int_{R_\mathrm{c}}^{R_\mathrm{e}} \varrho_\mathrm{e} 4\pi r^2 \,\mathrm{d}r = \frac{4\pi}{3} \left(R_\mathrm{e}^3 - R_\mathrm{c}^3\right) \varrho_\mathrm{e} = \frac{4\pi}{3} R_\mathrm{e}^3 \varrho_\mathrm{g} \,. \tag{15}
$$

This is a differential equation for R_e: With ϱ_e taken from (14) we can resolve it for $\dot{R}_\mathrm{e}$ and also find v_{R_e}:

$$
\dot{R}_\mathrm{e} = c_\mathrm{g} \left(1 - \frac{\gamma_\mathrm{g}+1}{2} \left(\frac{R_\mathrm{c}}{R_\mathrm{e}}\right)^3\right)^{-1/2}, \quad v_{R_\mathrm{e}} = \dot{R}_\mathrm{e} \left(\frac{R_\mathrm{c}}{R_\mathrm{e}}\right)^3 \,. \tag{16}
$$

The energies of SWe are given by:

$$
\begin{aligned}
E_\mathrm{ek} &\equiv \int_{R_\mathrm{c}}^{R_\mathrm{e}} \varrho_\mathrm{e} \frac{v_\mathrm{e}^2}{2} 4\pi r^2 \,\mathrm{d}r = \frac{4\pi}{3} \frac{\varrho_\mathrm{g}}{6} \left(R_\mathrm{e}^3 \dot{R}_\mathrm{c}^2 + R_\mathrm{c}^3 \dot{R}_\mathrm{c} \dot{R}_\mathrm{e} + \frac{R_\mathrm{c}^6}{R_\mathrm{e}^3} \dot{R}_\mathrm{e}^2\right) \\
E_\mathrm{et} &\equiv \int_{R_\mathrm{c}}^{R_\mathrm{e}} \frac{p_\mathrm{e}}{\gamma_\mathrm{g}-1} 4\pi r^2 \,\mathrm{d}r - E_{\mathrm{et\ ambient}} \\
&= \frac{4\pi}{3} \left(R_\mathrm{e}^3 - R_\mathrm{c}^3\right) \frac{p_\mathrm{c}}{\gamma_\mathrm{g}-1} - \frac{4\pi}{3} R_\mathrm{e}^3 \frac{p_\mathrm{g}}{\gamma_\mathrm{g}-1} \,.
\end{aligned} \tag{17}
$$

The last expression for $E_{\rm ek}$ is an approximation, with an accuracy of about 20% as long as $R_{\rm e}/R_{\rm c} < 2$. $E_{\rm et}$ is the *excess* thermal energy in the SWe. The subtraction of the ambient thermal energy is essential for the description of plume stopping. Within similar approximations, the momentum $P_{\rm e}$ is:

$$P_{\rm e} \equiv \int_{R_{\rm c}}^{R_{\rm e}} \varrho_{\rm e} v_{\rm e} 4\pi r^2 \,{\rm d}r = \frac{4\pi}{3}\frac{\varrho_{\rm g}}{2}\left(R_{\rm e}^3\dot{R}_{\rm c} + R_{\rm c}^3\dot{R}_{\rm e}\right) . \qquad (18)$$

This allows one to find the pressure $p_{\rm c}$ from (5), which then can be substituted into (13) and (17).

$$p_{\rm c} \equiv \frac{\dot{P}_{\rm e}}{4\pi R_{\rm c}^2} + \left(\frac{R_{\rm e}}{R_{\rm c}}\right)^2 = \frac{\varrho_{\rm g}}{6R_{\rm c}^2}\frac{\rm d}{{\rm d}t}\left[R_{\rm e}^3\dot{R}_{\rm c} + R_{\rm c}^3\dot{R}_{\rm e}\right] + \left(\frac{R_{\rm e}}{R_{\rm c}}\right)^2 p_{\rm g} . \qquad (19)$$

Note that the first equality is this equation is *exact*.

3 Results and discussion

The temporal behavior of radii $R_{\rm i}$, $R_{\rm c}$, $R_{\rm e}$, and R obtained from the numerical solution of (1)–(6) is shown in Fig. 2. It is instructive to study this picture in conjunction with Fig. 3, in which the transformation of energies between the plume and SWs is shown. One can see how the initial inertial expansion $R \propto t$ slows down because of snow-plowing of ambient gas in the SWe. SWi is simultaneously formed, and initially it propagates close to contact surface. At this stage, all energy is in the kinetic energy of the (almost free) plume. With $M_{\rm e} \sim M$, SWi becomes wider, moves inward, and reaches the center; it already possesses noticeable percentage of kinetic energy. Later, the *homogeneous* plume is characterized by $E_{\rm ik}$ and $E_{\rm it}$. Simultaneously, kinetic and thermal energy of SWe builds up; later $R_{\rm c}$ and $R_{\rm e}$ propagate close to each other according to point-blast law: $R \propto t^{2/5}$. Here, thermal energy is mainly within the plume, while kinetic energy is mainly within the SWe as $M_{\rm e} \gg M$. The plume is not completely adiabatic at this stage. Though here we describe this by the

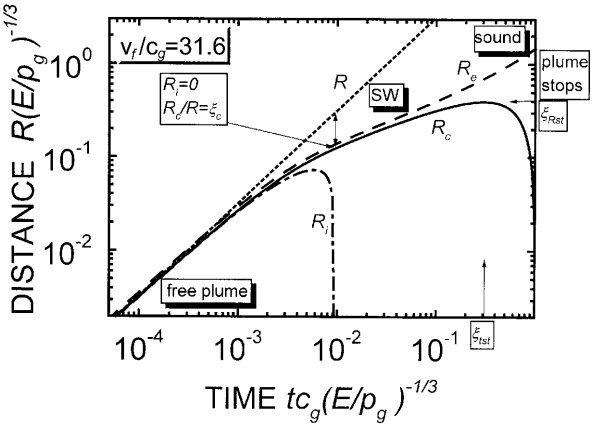

Fig. 2. Dynamics of plume expansion in dimensionless variables. *Dotted line*: free plume R; *dash-dotted line*: internal SW $R_{\rm i}$; *solid line*: contact boundary $R_{\rm c}$; *dashed line*: external SW $R_{\rm e}$. Dimensionless coefficients, which characterize turnover and stopping points (for high $v_{\rm f}/c_{\rm g}$ ratio) are given in Table 1. Parameters: $\gamma_{\rm p} = 5/3$, ($\gamma_{\rm g} = 5/3, k = 1/(\gamma_{\rm p} - 1) = 3/2$. Free-plume expansion velocity is such that $(v_{\rm f}/c_{\rm g})^2 = 10^3$

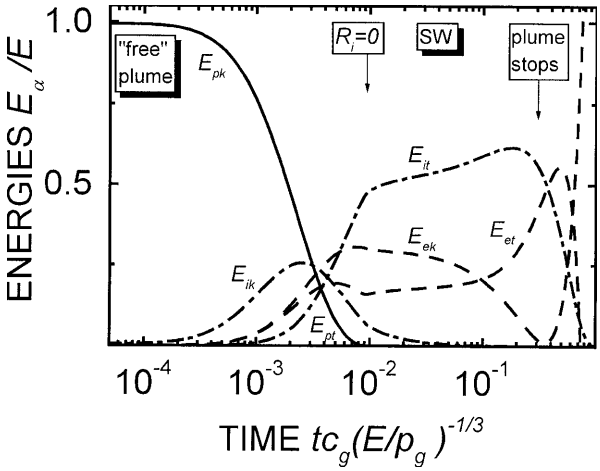

Fig. 3. Redistribution of kinetic and thermal energies (indexes k and t, respectively) between the plume and external SW in the course of expansion. All energies are normalized to initial energy E. *Solid lines*: central part of the plume ($E_{\rm pk}$ and $E_{\rm pt}$). $E_{\rm pk}$ is small everywhere. *Dash-dotted lines*: internal SW, later the whole homogenized plume ($E_{\rm ik}$ and $E_{\rm it}$). *Dotted lines*: external SW ($E_{\rm ek}$ and $E_{\rm et}$). Parameters are as in Fig. 2

averaged description, in reality it is due to oscillating SWi. As long as SWe remains strong, all energies are almost constant. The width of the SW region depends on the single parameter $v_{\rm f}/c_{\rm g}$. However, even for rather high initial velocity $v_{\rm f}$ used in Figs. 2 and 3, the finite pressure of ambient gas soon results in the stopping of the plume, accompanied by its additional heating. The SWe detaches from the contact surface and becomes a sound wave ($R_{\rm e}$ approaches slope 1 in Fig. 2). At this stage, $E_{\rm ek}$ naturally decreases, while $E_{\rm et}$ increases. After the stopping point, the model does not work, because of inadequate description of the velocity distribution in the detached *weak* SWe. Below we discuss simplified expressions for different transitional stages.

3.1 Homogenization of the plume

After the SWi reaches the center, we treat the plume as homogeneous. All of the plume is then described as "internal SW". This happens when the mass of SWe becomes comparable with that of the plume, as SWi develops because of the presence of ambient gas. Thus, $R_{\rm i} = 0$ occurs near the turnover between free expansion and strong-SW propagation regimes. We introduce several dimensionless coefficients, which characterize the point $R_{\rm i}$:

$$R_{\rm i} = \zeta_{\rm i}\left(\frac{M}{\varrho_{\rm g}}\right)^{1/3}, \; t_{\rm i} = \zeta_{\rm ti}\left(\frac{M^5}{E^3\varrho_{\rm g}^2}\right)^{1/6}, \; \zeta_M \equiv \frac{M_{\rm e}}{M}, \; \zeta_{\rm c} \equiv \frac{R_{\rm c}}{R} , \qquad (20)$$

$\zeta_{\rm c}$ is found analytically from (12) with the first term $M_{\rm p} = 0$, and $R_{\rm i} = 0$. The point $R_{\rm i} = 0$ can be found graphically. One can draw the line $\zeta_{\rm c} R$ using the initial slope of expansion; its intersection with the (measured) $R_{\rm c}$ dependence yields the time (and $R_{\rm c}$) when $R_{\rm i} = 0$.

3.2 Homogeneous plume, strong external SW

After the homogenization, the expansion equations can be simplified. If one is not interested in the internal structure of the plume, this is a good approximation even at the initial stage. For *strong* SWe, (16) yields:

$$R_{\rm e} = \left(\frac{\gamma_{\rm g}+1}{2}\right)^{1/3} R_{\rm c} \,. \tag{21}$$

Substituting this into (17)–(18), we obtain:

$$E_{\rm ek} = \zeta_E \frac{4\pi}{3} R_{\rm c}^3 \varrho_{\rm g} \frac{\dot{R}_{\rm c}^2}{2} \,, \qquad E_{\rm et} = \frac{4\pi}{3}\frac{R_{\rm c}^3}{2}\left(p_{\rm c} - \frac{\gamma_{\rm g}+1}{\gamma_{\rm g}-1} p_{\rm g}\right) \,,$$
$$P_{\rm e} = \zeta_P \frac{4\pi}{3} R_{\rm c}^3 \varrho_{\rm g} \dot{R}_{\rm c} \,. \tag{22}$$

The coefficients ζ_E and ζ_P are slightly bigger than 1 as $R_{\rm e} > R_{\rm c}$. More detailed consideration yields similar expressions $\zeta_E, \zeta_P \sim 1$. This holds even with $\varrho_{\rm e} \neq const$. Using (22) for the pressure $p_{\rm c}$ in (19), substituting into the energy conservation (4), and rearranging, we get:

$$\left(\frac{3}{10}M + \frac{\zeta_A}{\gamma_{\rm g}} R_{\rm c}^3 \varrho_{\rm g}\right) \dot{R}_{\rm c}^2 + \frac{\zeta_B}{\gamma_{\rm g}} R_{\rm c} \varrho_{\rm g} \frac{{\rm d}}{{\rm d}t}\left[R_{\rm c}^3 \dot{R}_{\rm c}\right] + \zeta_{\rm C} R_{\rm c}^3 p_{\rm g} = E \,. \tag{23}$$

Substitution $p(R_{\rm c}) = {\rm d}R_{\rm c}/{\rm d}t$ results in a linear equation $f(R_{\rm c})\,{\rm d}R_{\rm c} = {\rm d}t$. The integration cannot be carried out, however. Below we study two transitional regions.

3.3 Free expansion–strong-SW transition

In the region where $p_{\rm c} \gg p_{\rm g}$, the last term in the l.h.s. of (23) is unimportant. With $R_{\rm c} \propto (t-t_0)^n \Rightarrow R_{\rm c}^3 \dot{R}_{\rm c}^2 = (4 - \frac{1}{n}) R_{\rm c} \frac{\rm d}{{\rm d}t}\left[R_{\rm c}^3 \dot{R}_{\rm c}\right]$; n changes from $n=1$ at the initial stage of expansion to $n = 2/5$ at the strong-SW stage. Initially, terms involving $R_{\rm c}^3$ are small in comparison with $M\dot{R}_{\rm c}^2$ anyway. If we assume $n \approx 2/5$, the solution of resulting equation can be expressed via the incomplete beta function B:

$$\tau = -\frac{1}{3} B_{-\mathcal{R}^3}\left(\frac{1}{3}, \frac{3}{2}\right), \qquad R_{\rm c} \equiv \zeta_{R_{\rm SW}} \left(\frac{M}{\varrho_{\rm g}}\right)^{1/3} \mathcal{R},$$
$$r \equiv \zeta_{t_{\rm SW}} \left(\frac{M^5}{\varrho_{\rm g}^2 E^3}\right)^{1/6} \tau \,. \tag{24}$$

3.4 Stopping distance

With $p_{\rm c} \sim p_{\rm g}$ in the course of expansion, the plume stops, because of the last term in (23). Though SWe is not strong at this stage, (23) qualitatively describes the way the plume decelerates. In the stopping region, kinetic energy of the plume (first term in brackets in (23)) can be neglected. Then (23) can be simplified, and its solution can be written as:

$$\tau = \frac{1}{3} B_{\mathcal{R}^3}\left(\frac{5}{6}, \frac{1}{2}\right), \quad R_{\rm c} \equiv \zeta_{R_{\rm st}} \left(\frac{E}{p_{\rm g}}\right)^{1/3} \mathcal{R},$$
$$t \equiv \zeta_{t_{\rm st1}} \left(\frac{E}{p_{\rm g}}\right)^{1/3} \frac{\tau}{c_{\rm g}} \,. \tag{25}$$

Within this approximation, the plume stops at:

$$\mathcal{R} = 1, \quad \tau = \frac{1}{3} B_1\left(\frac{5}{6}, \frac{1}{2}\right) \approx 0.75 \,. \tag{26}$$

Thus, stopping distance is characterized by $\zeta_{R_{\rm st}}$, and stopping time by $\zeta_{t_{\rm st}} \approx 0.75 \zeta_{t_{\rm st1}}$. The values of $\zeta_{R_{\rm st}}$ and $\zeta_{t_{\rm st}}$ (see Table 1) found *numerically* are significantly lower, as (weakened) SWe occupies a much larger volume than that assumed by the (21) and simplified equation (23). (Its radius is $\zeta_{\rm e}$ times bigger than the contact surface).

3.5 Comparison with experiment

Figure 4 shows the results obtained with steel and $YBa_2Cu_3O_{7-x}$ (YBCO) with different Ar pressures p and laser energies E. A KrF Lambda Physics excimer laser (wavelength $\lambda = 248$ nm, $t_{\rm FWHM} \approx 30$ ns), spot size (top hat) ($2w \approx 1$ mm) was used. The visible plume boundary was measured by a Photometrics gated ICCD camera. Agreement between theory and experiment was found to be good,

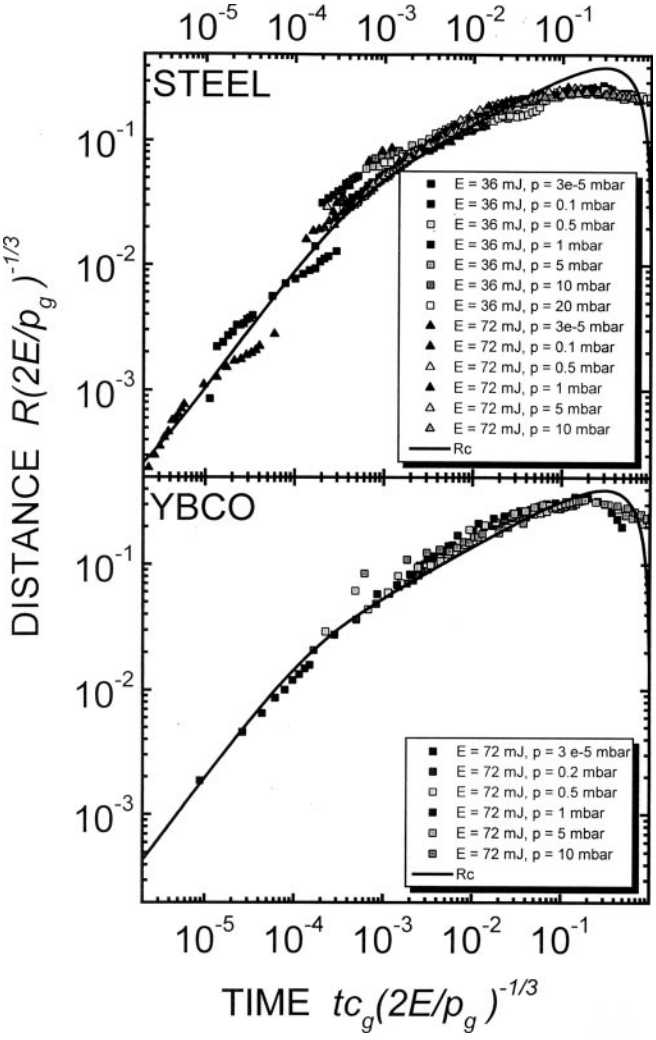

Fig. 4. Experimental data (*symbols*) for steel and YBCO in dimensionless variables. *Solid lines* are calculated with $v_{\rm f}/c_{\rm g} = 100$ for steel and $v_{\rm f}/c_{\rm g} = 200$ for YBCO. Other parameters are as in Fig. 2

though virtually *no fitting parameters* were used. The mass of the plume was taken from the expansion velocity at low pressures. One can clearly see the free expansion–strong-SW transition and stopping point. Their positions (especially for stopping) are in good agreement with theory both in distance and time. Discrepancies may be due to nonspherical geometry of real expansion, losses of energy for sample heating, plasma radiation, or recombination processes. Deviations, noticeable for steel at low pressures, may be also due to difficulties in determination of the plume boundary in this region.

4 Conclusions

An analytical model for the spherical plume expansion into the ambient atmosphere has been presented. It covers almost-free initial expansion, strong-SW propagation in the intermediate stage, and plume stopping. Internal SW describes heating of the plume edge and plume splitting. Theoretical results are applied to the analysis of ablation of steel and YBCO in argon.

Acknowledgements. We are grateful to Professors S. Anisimov, D. Bäuerle, B. Luk'yanchuk, and Dr. N. Bityurin for useful discussions, and to Jubiläumsfonds der Österreichischen Nationalbank, projects #6806 and #7563, for financial support.

References

1. Y.B. Zeldovich, Yu.P. Raizer: *Physics of Shock Waves and High-Temperature Hydrodynamic Phenomena*, ed. by W.D. Hayes, R.F. Probstein (Academic Press, London 1966)
2. S.I. Anisimov, D. Bäuerle, B.S. Luk'yanchuk: Phys. Rev. B **48**, 12 076 (1993)
3. L.I. Sedov: *Similarity and Dimensional Methods in Mechanics* (Academic Press, London 1959)
4. J.L. Giuliani, Jr., M. Mulbrandon, E. Hyman: Phys. Fluids B [Plasma Physics] **1**(7), 1463 (1989)
5. F. Garrelie, C. Champeaux, A. Catherinot: Appl. Phys. A **69**, 45 (1999)
6. A.V. Bulgakov, N.M. Bulgakova: J. Phys. D: Appl. Phys. **28** (8), 1710 (1995)
7. D.B. Geohegan: In *Excimer Lasers*, ed. by L.D. Laude, NATO ASI Series, Vol. E 256 (Kluwer Academic Publishers, Dordrecht 1994) p. 165
8. R.F. Wood, J.N. Leboeuf, D.B. Geohegan, A.A. Puretzky, K.R. Chen: Phys. Rev. B **58** (3), 1533 (1998)
9. S.I. Anisimov, Ya. B. Zel'dovich: Sov. Tech. Phys. Lett. **3** (10), 445 (1977)
10. J.N. Leboeuf, R.F. Wood, K.R. Chen, A.A. Puretzky, D.B. Geohegan: Phys. Rev. Lett. **79** (8), 1571 (1997)
11. K.P. Stanyukovich: *Unsteady Motion of Continuous Media* (Pergamon, London 1960)
12. M.R. Predtechensky, A.P. Mayorov: Appl. Supercond. **1** (10–12), 2011 (1993)
13. J.L. Bobin, Y.A. Durand, Ph.P. Langer, G. Tonon: J. Appl. Phys. **39** (9), 4184 (1968)
14. O.B. Anan'in, Yu.A. Bykovskii, Yu.V. Eremin, E.L. Stupitskii, I.K. Novikov: Sov. J. Quantum. Electron. **QE-21** (7), 787 (1995)